

The influence of secondary electron emission on a capacitive chlorine discharge

B. Mahdavi¹ and J. T. Gudmundsson^{1,2}

¹Science Institute, University of Iceland, Reykjavík, Iceland

²Division of Space and Plasma Physics, KTH Royal Institute of Technology, Stockholm, Sweden



Abstract

We apply particle-in-cell Monte Carlo collision simulations to study the impact of secondary electron emission on a capacitively coupled chlorine discharge in the pressure range 2–50 Pa. At a pressure of around 20 Pa striations appear. In particular we explore how secondary electron emission influences the striations.

Introduction

The particle-in-cell Monte Carlo code oopd1 is used to study a capacitively coupled chlorine discharge with Cl_2 as the feedstock gas.

The model includes various species, such as $\text{Cl}_2(X^1\Sigma_g^+, v=0)$, $\text{Cl}(^2P_{1/2})$, $\text{Cl}^-(^1S_g)$, $\text{Cl}^+(^3P_g)$, and $\text{Cl}_2^+(^2\Pi_g)$ [1] and this model has been used in recent studies of the capacitive chlorine discharge [2, 3].

Here, we upgrade and compare the cross sections for electron impact excitation and dissociation from Rescigno [4] (old) to the more recent calculations of Hamilton et al. [5] (new).

The discharge is driven by a sinusoidal rf voltage with an amplitude of 222 V across a 2.54 cm gap.

Secondary electron emission yields for ion-induced and ground state atom-induced electron emission are considered using fits for argon ions and argon atoms from Phelps and Petrović [6].

Electron-induced secondary electron emission is accounted for using Vaughan's formula [7] or the modified Vaughan's formula as discussed by Wen et al. [8].

We compare five cases, two that neglect secondary electron emission, and three with varying electron emission processes as can be seen in the table below.

| Case | neutrals | ions | electrons |
|------|--|--|--|
| I | 0.0 | 0.0 | 0.0 |
| II | 0.0 | 0.0 | 0.0 |
| III | $\gamma_{\text{sec},n}(\mathcal{E}_n)$ | $\gamma_{\text{sec},i}(\mathcal{E}_i)$ | 0.0 |
| IV | 0.0 | 0.5 | 0.0 |
| V | $\gamma_{\text{sec},n}(\mathcal{E}_n)$ | $\gamma_{\text{sec},i}(\mathcal{E}_i)$ | $\gamma_{\text{sec},e}(\mathcal{E}_e, \theta)$ |

Results and discussion

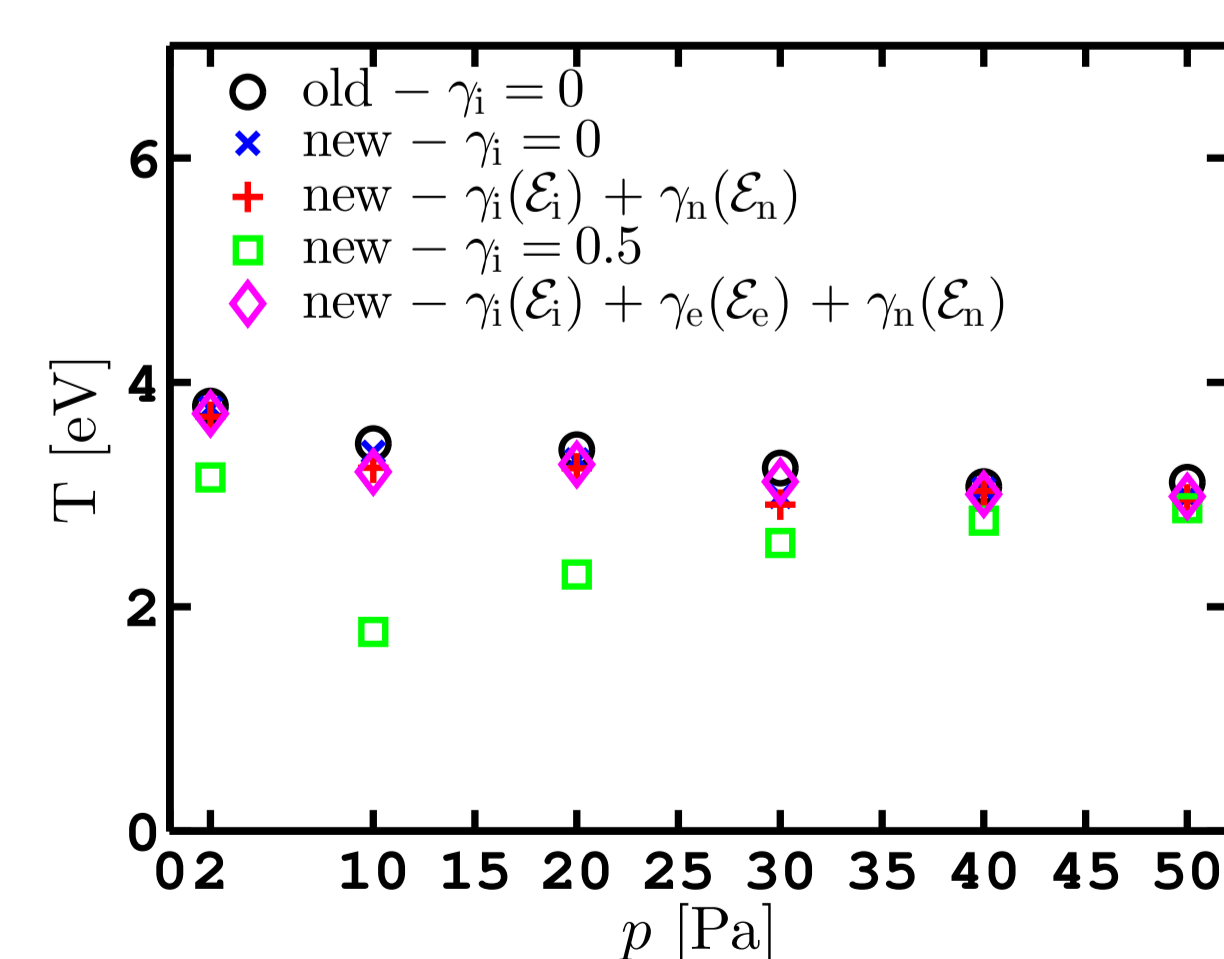


Figure 1: The time averaged electron temperature at the discharge center versus pressure for different secondary emission conditions.

The electron temperature in the discharge center is shown versus pressure – at the pressure of 2 Pa, all cases exhibit the same electron temperature, except case IV (with high ion induced secondary electron emission) that exhibits a lower electron temperature.

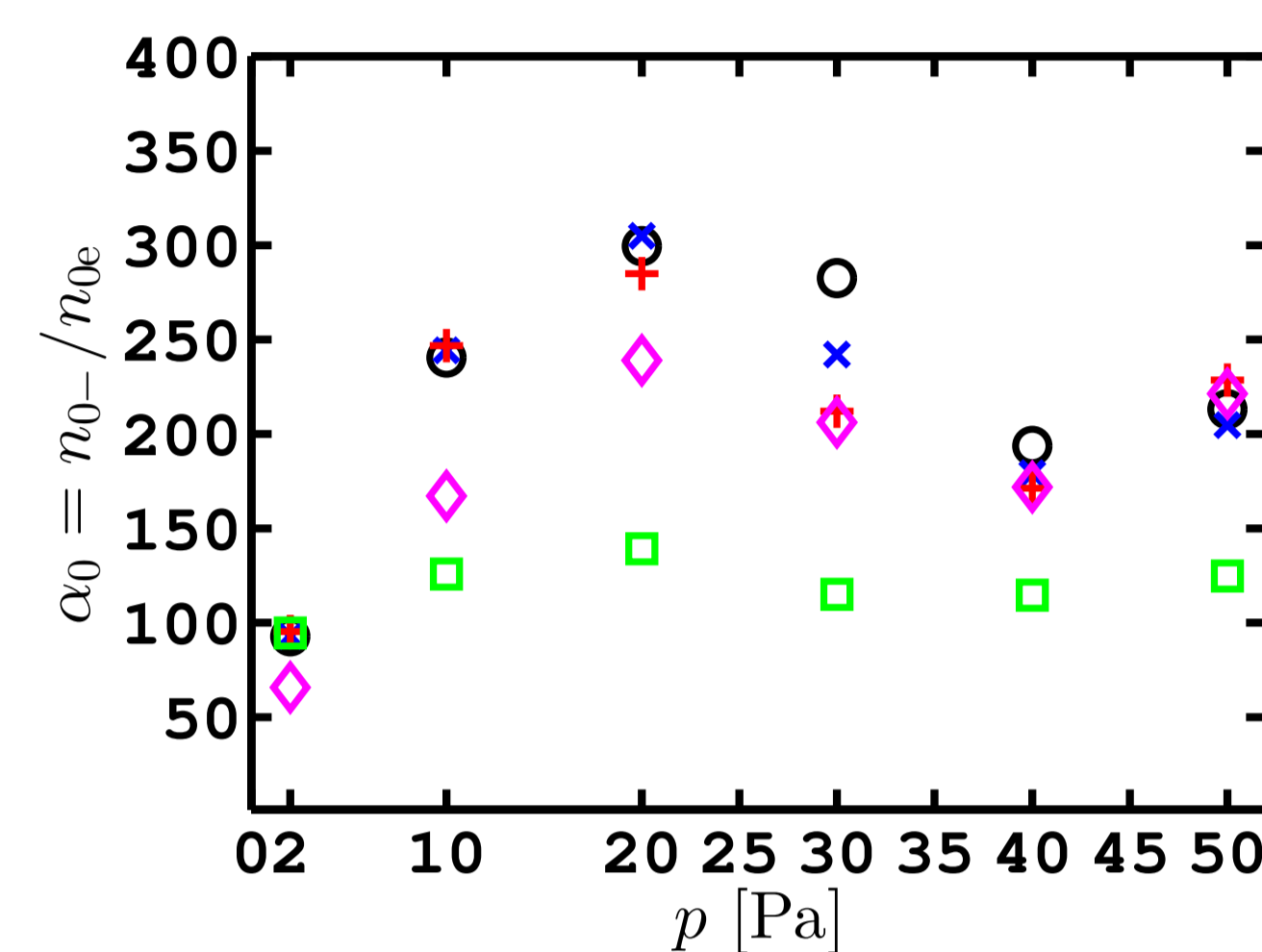


Figure 2: The electronegativity α_0 at the discharge center versus pressure for different secondary emission conditions.

Figure 2 shows the electronegativity in the discharge center versus pressure.

As the pressure increases, all cases demonstrate a similar trend: an initial increase in electronegativity up to 20 Pa, followed by a decrease between 20–40 Pa, and a slight increase thereafter – case IV (high ion induced secondary electron emission yield) has lower electronegativity than other cases above 10 Pa.

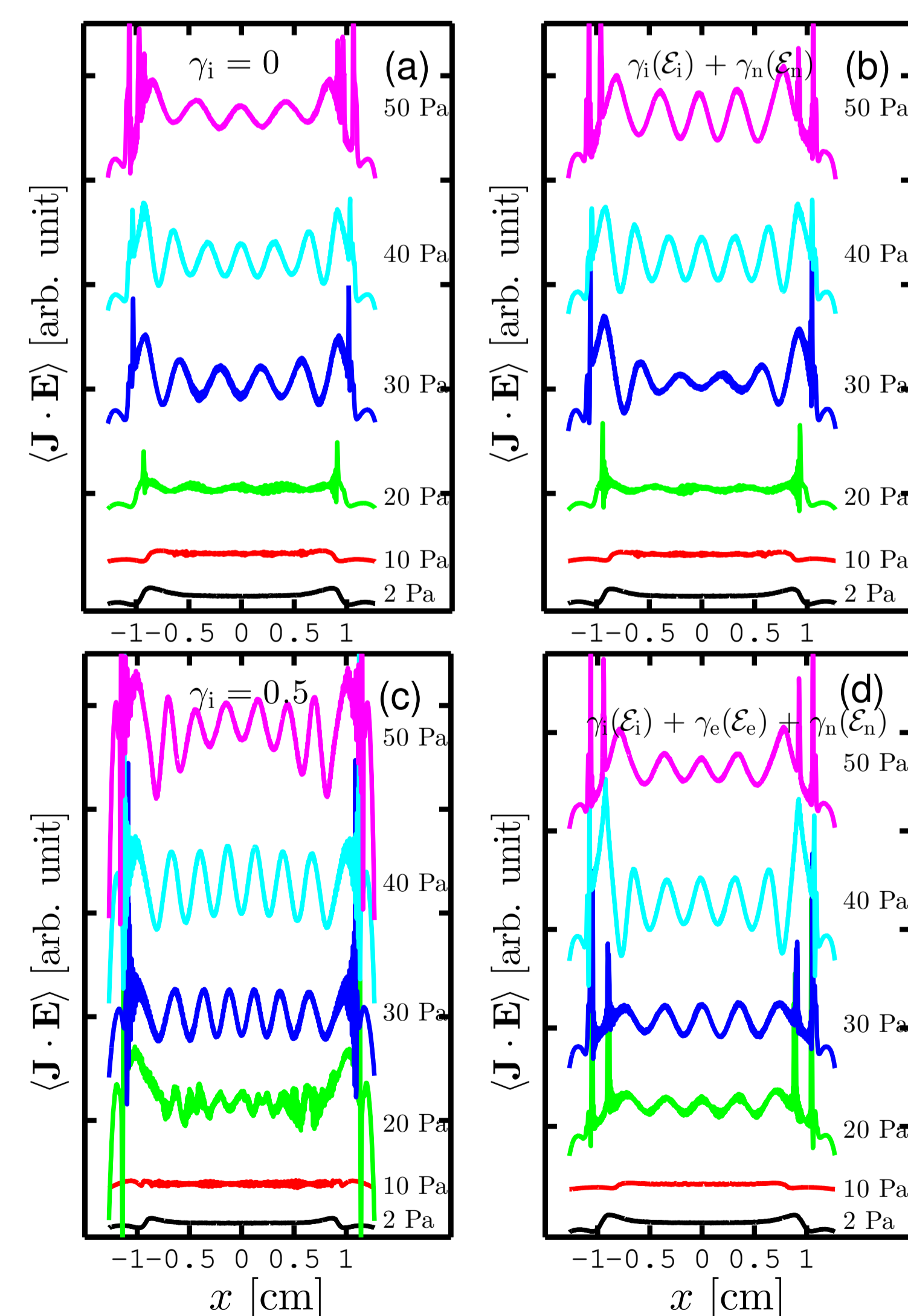


Figure 3: Electron power absorption in different pressures for (a) case II, (b) case III, (c) case IV, and (d) case V.

Striations have been observed in the capacitive chlorine discharge for pressure above 20 Pa [2, 3].

Figure 3 demonstrates the electron power absorption in the pressure range 2–50 Pa for varying secondary emission conditions.

We see that for all cases, the transition to striations starts at 20 Pa, where during one rf period electrons cross multiple striation gaps in the bulk region.

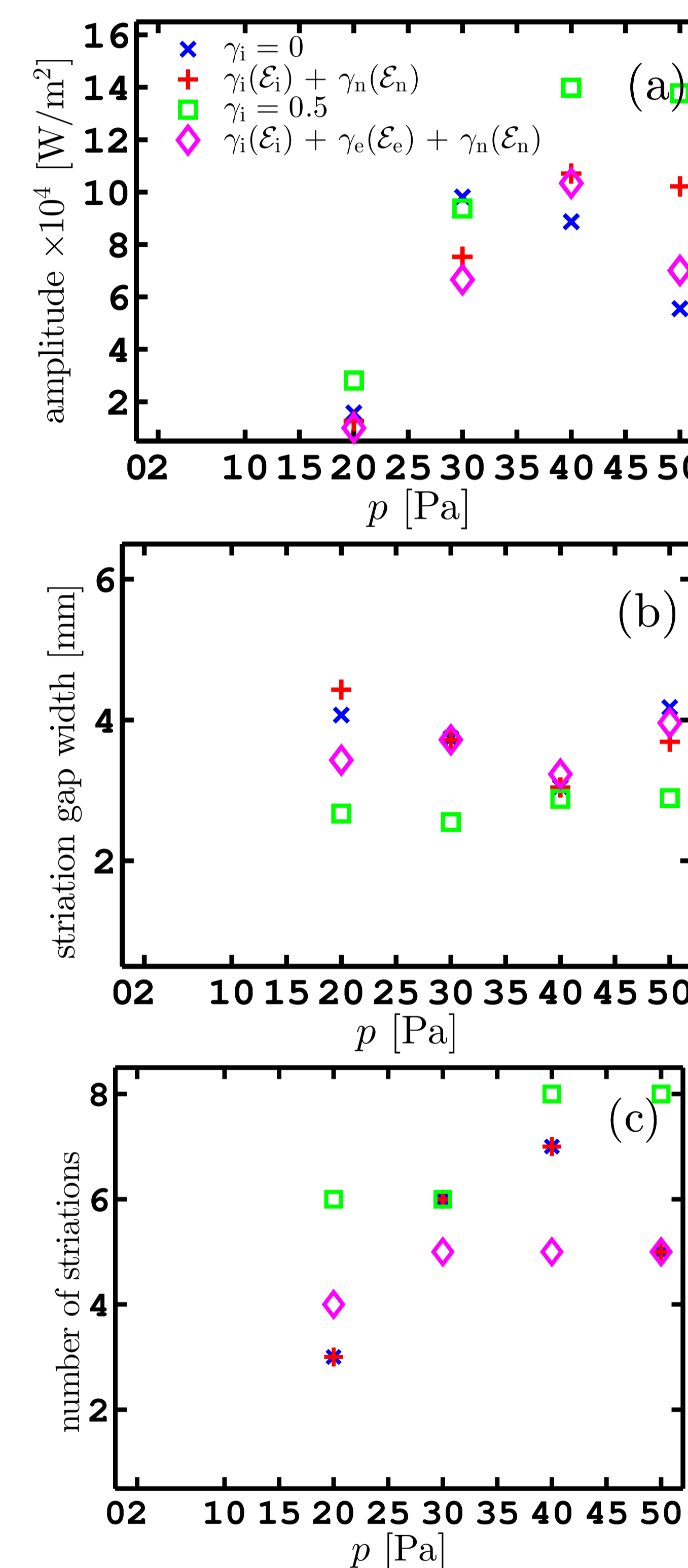


Figure 4: (a) Averaged striation peak to peak electron power absorption at the discharge center, (b) averaged striation gap width at the discharge center, and (c) number of striations, versus the pressure for various secondary electron emission processes (cases II–V).

Figure 4 (a) shows the peak-to-peak power absorption of the striations versus pressure. It can be observed that the averaged striation amplitude exhibits a pattern of initial increase with increased pressure followed by a decrease with further increase in pressure for all cases.

Figure 4 (b) shows the average striation gap width versus pressure for varying completeness of the secondary electron emission processes.

At 20 Pa, case II (no secondary electron emission) has the longest gap width, while case IV (very high ion induced secondary electron emission) has the shortest.

At 50 Pa, the striation gaps widen for all cases except case IV, which remains relatively unchanged.

Figure 4 (c) displays the number of striations for each case – cases II and III exhibit a similar trend, with an increase in the number of striations up to 40 Pa, followed by a decrease for pressure above 40 Pa.

For case V (the most complete model for secondary electron emission), there is a slight increase at 30 Pa, while the number of striations remains constant until 50 Pa.

Notably, case IV consistently has the highest number of striations across all pressure values.

Conclusions

We have applied one-dimensional particle-in-cell Monte Carlo collisional (PIC/MCC) simulations of capacitive chlorine discharges in the pressure range of 2–50 Pa, varying the secondary electron emissions processes.

With increasing pressure, all cases show a similar pattern in electronegativity: an initial rise up to 20 Pa, followed by a decline in the pressure range 20–40 Pa, followed by a slight increase with further increase in pressure.

The case with the highest ion-induced secondary electron emission exhibits the lowest electronegativity.

Both the pressure and the secondary electron emission, have an influence on the discharge electrogenativity and the electron temperature as well as the striation structure.

References

- [1] S. Huang and J. T. Gudmundsson. *Plasma Sources Sci. Technol.*, **22**(5), 055020, 2013.
- [2] G. A. Skarphedinsson and J. T. Gudmundsson. *Plasma Sources Sci. Technol.*, **29**(8), 0845004, 2020
- [3] A. Proto and J. T. Gudmundsson. *Plasma Sources Sci. Technol.*, **30**(6), 065009, 2021
- [4] T. N. Rescigno. *Phys. Rev. A*, **50**(2), 1382–1389, 1994.
- [5] J. R. Hamilton et al. *Plasma Sources Sci. Technol.*, **27**(9), 095008, 2018.
- [6] A. V. Phelps and Z. L. Petrovic. *Plasma Sources Sci. Technol.*, **8**(3), R21–R44, 1999.
- [7] R. M. Vaughan. *IEEE Trans. Electron Devices*, **36**(9), 1963–1967, 1989.
- [8] D.-Q. Wen et al. *Plasma Sources Sci. Technol.*, **32**(3), 064001, 2023.